IEEE Access
Multidisciplinary | Rapid Review | Open Access Journal

Received February 21, 2020, accepted March 2, 2020, date of publication March 12, 2020, date of current version March 20, 2020.

Digital Object Identifier 10.1109/ACCESS.2020.2980251

Improved EXIT Algorithm Based on Gaussian Mixture Model and Its Application to LDPC Construction in Coding Cooperative Systems With Hybrid Fading

ZHIXIONG CHEN, YU GU, PEIRU CHEN, JINGXI ZHANG, AND DONGSHENG HAN
School of Electrical and Electronic Engineering, North China Electric Power University, Baoding 071000, China

Corresponding author: Zhixiong Chen (zxchen@ncepu.edu.cn)

This work was supported in part by the National Natural Science Foundation of China under Grant 61601182 and Grant 61771195, in part by the Natural Science Foundation of Hebei Province under Grant F2017502059 and Grant F2018502047, and in part by the Fundamental Research Funds for the Central Universities under Grant 2019MS088.

ABSTRACT In this study, an EXIT algorithm based on Gaussian mixture coding and multi-dimensional node information calculation is proposed. The objective is to solve the problem of performance analysis of cooperative communication and LDPC code construction under hybrid fading and impulse noise. First, Gaussian mixture model estimation of the decoding initialization information is performed by the expectation maximized algorithm. In addition, key parameters, such as weight, mean, and variance of the Gaussian mixture model are obtained. Then, the multi-dimensional information processing is performed on the variable node and the check node information in the traditional EXIT algorithm based on the multi-dimensional Gaussian mixture model and system symmetry analysis. Finally, the objective function of LDPC code optimization is constructed, the constraints are given, and the optimal LDPC code degree distribution is obtained by the differential evolution algorithm. The simulation results show that compared with the traditional regular and other irregular LDPC codes, the newly constructed degree distribution has better performance in waterfall characteristics and error floor characteristics. Such distribution provides a necessary method to analyze and optimize the performance of cooperative coding system under hybrid media or hybrid fading.

INDEX TERMS Expectation maximization (EM), Gaussian mixture, hybrid fading, low-density parity-check (LDPC) codes, multi-dimensional EXIT.

I. INTRODUCTION

Power line communication (PLC) and wireless communication technologies have broad application prospects in networking represented by smart grids and homes [1]–[4]. PLC delivers information through the existing power line infrastructure without re-laying lines, requiring fewer deployment costs [5]. However, realizing reliable transmission of long distances of power lines is a challenge because of the effects of impulse noise and fading [6]. Wireless communication has the advantages of flexible access and simple networking [7] but high-frequency signals, such as 2.4 and 5.8 GHz have large attenuation and are easily blocked by obstacles. Wireless communication, PLC, and other communication methods have their own characteristics. The combined power line and wireless dual-media parallel communication technology can integrate resources, complement each other, save construction costs, and improve overall system performance [8]. Cooperative communication technology is one of the hotspots in academic research as an effective means of anti-fading and improving the reliability of communication systems. In terms of cooperative communication, PLC technology based on a multi-hop relay, dual media parallel communication, and joint decoding has gradually become an important research content.

Exploring the relay forwarding in PLC applications, Dubey *et al.* analyze the system performance of PLC using amplify and forward (AF) [9] and decode and forward

The associate editor coordinating the review of this manuscript and approving it for publication was Faissal El Bouanani.

This work is licensed under a Creative Commons Attribution 4.0 License. For more information, see https://creativecommons.org/licenses/by/4.0/

(DF) [10] relays. In [11], an energy allocation algorithm in multi-base-station collaboration system is studied. The relay node can improve the energy efficiency of the power line relay system effectively through energy collection and effective power allocation strategy. The experimental results proved that the algorithm can balance the time-of-use power price of a smart power grid and the energy storage of a base-station. Reference [12] gives an expression of channel capacity for multi-hop relay technology based on AF protocol in power line access networks. In [13], the system capacity of the two-hop relay PLC system using orthogonal frequency division multiplexing modulation under AF and decoding and forward (DF) protocols are analyzed. Cheng *et al.* [14] use multipath and transmission line theory models to study the capacity limit and optimal power allocation of the PLC system based on AF protocol under power bandwidth limitation. Reference [15] analyzes the system performance of PLC after network coding but does not consider the impact of impulse noise. The above research shows that the use of relay technology can improve the long-distance communication capability of PLC systems.

The latest research hotspots model power line channel fading into a lognormal (LogN) model [16]. In [9], the effect of AF forwarding on the average channel capacity in the PLC channel is studied based on Bernoulli-Gaussian impulse noise and fading. Furthermore, the approximate closed-form expression of the bit error rate (BER) and the average channel capacity at high signal to noise ratio are given. Reference [17] deduces the system error rate, channel capacity, and outage probability expression when the system adopts DF relay and multihop based on the power line channel of lognormal fading and Bernoulli–Gaussian impulse noise. The above studies all use the Bernoulli–Gaussian model to model the impulse noise in the channel, which is more concise and intuitive compared with the Middleton-A model. However, these studies do not involve wireless communication cooperation and do not consider the problem of wireless access to mobile terminals.

On the research of power line and wireless parallel communication system, [18] proposes a system structure of wireless and power line parallel communication. Furthermore, such study derives the BER performance in the presence of impulse noise but sets the fading coefficient of the power line to a fixed constant. Lai and Messier [19] verify the complementarity between PLC and wireless communication through measured data and achieve significant diversity gain by selection combining (SC) and maximum ratio combining (MRC). In [20], the two-hop relay technology of parallel communication between wireless and PLC is studied. The channel adopts deterministic complex fading coefficient, and the diversity of branches does not consider the influence of impulse noise. In [21], the problem that the theoretical performance of amplify-and-forward relay communication based on hybrid fading condition has no closed expression in ower line and wireless hybrid communication system is studied. The mixture LogN approximate algorithm based on moment-generating function is applied to approximate a wireless fading coefficient to mixture LogN distribution. The above research focuses on the diversity and algorithm and system performance analysis under heterogeneous media. No specific research on key technologies, such as resource allocation and joint coding modulation in parallel communication exists.

Advanced channel coding techniques, such as turbo code and low-density parity-check (LDPC) code can be applied to PLC to improve communication reliability because the power line channel is affected by impulse noise and multipath fading [9]. The IEEE 1901 Working Group proposes the use of a turbo code-based coding scheme, but such scheme requires a large amount of turbo code patent fees. The theory verifies the great potential of LDPC codes in PLC [22], and the ITU G.hn standard recommends the use of LDPC codes as the channel coding scheme of PLC [23]. Reference [24] deduces the BER performance of the wired communication domain such as power line and twisted pair under the G.hn standard using bidirectional PLNC. The above study focuses mainly on the application of LDPC codes in PLC and its simulation performance and has not solved the problem of coding design and code optimization for impulse noise. Iterative decoding performance analysis and code optimization under the mixed noise and dual-medium mixed fading environment have certain challenges.

The traditional LDPC code iterative decoding performance analysis methods include density evolution, Gaussian approximation, and EXIT charts. The Gaussian approximation and the EXIT algorithm use the Gaussian distribution of the log-likelihood ratio (LLR) of the decoder and the relationship that the variance is twice the mean to simplify the algorithm complexity. The forms of fading and noise in different media channels are often different in the dual media cooperative communication system. In particular, the power line channel noise has a pulse characteristic and no longer satisfies the Gaussian distribution. Traditional algorithms such as EXIT charts are not suitable for use in power line-wireless dual media cooperative communication systems. Hence, traditional EXIT charts need to be appropriately improved and optimized. For the impulse noise interference system such as shallow water acoustic communication, [25] adopts the symmetric and stable distribution of impulse noise model and optimizes and designs the degree distribution of LDPC code by using EXIT chart and quantization density evolution. Reference [26] proposes combining spatial diversity with LDPC codes to obtain diversity gain based on channels with Rayleigh fading and symmetrically stable impulse noise. The coding performances of the linear diversity combining schemes of MRC, SC, and equal gain combining are studied. The progressive performance of LDPC codes is derived by density evolution. At the same time, the closed expression of the LDPC code waterfall performance is given to reduce the gap between the actual progressive performance of the LDPC code and the simulation. In [27], an optimization scheme for maximizing system throughput by changing the puncturing coefficient and mapping method is proposed for the changing

channel conditions in the FSO/RF system. The VND curve in the EXIT chart is related to the puncturing coefficient and the mapping scheme, and the CND curve has a relatively fixed relationship to satisfy the constraint of the EXIT chart convergence. The throughput of the system is maximized by changing the puncturing coefficient and the mapping scheme. In [28], the patent proposes a method for adaptively coding signals in optical network, which provides parametric analysis of nonlinear channel statistics by using Gaussian Mixture (GM) model. For the 2-user Gaussian Multiple Access Channel in [29], the EXIT functions of the multi-user decoder are proposed based on two different approximations of the DE. Besides, the stability condition and the optimization constraints is analyzed. In [30], the coding design of dual-user Gaussian multiple-access channel with fixed channel gain and quasi-static fading is studied. The stability conditions of LDPC codes in multi-user scenarios are derived based on the model of soft information exchange between two user LDPC code decoders using parallel transmission mode. The Gaussian mixture (GM) is used to obtain the probability density function (PDF) of the state node output LLR of the joint decoder. Improved density evolution and EXIT chart are proposed to analyze and construct LDPC codes for dual-user Gaussian multiple access channels by tracking the changes of PDF when LLR is exchanged in nodes. In [31], an improved scheme is proposed based on the dynamic characteristics in the decoding process and the non-Gaussian in information decoding, which improves the accuracy of the PDF and EXIT calculation of the GM estimation LLR. Finally, the modified EXIT chart is used to analyze the change of GM component in the iterative decoding process and construct a good performance LDPC code distribution. The above study uses the GM algorithm to analytically give the message PDF expression in the joint decoding process and improves the EXIT chart to improve the calculation accuracy. In [32], the EXIT charts are proposed to design non-binary low-density parity-check (LDPC) codes, where the priori information is modelled using a Gaussian mixture distribution. By matching the variable and check node EXIT curves, the method can design good non-binary LDPC for AWGN channel. Compared with the Turbo code, the high code rate can only be achieved by punching. The code rate of the LDPC code can be constructed arbitrarily and has greater flexibility. In the past, the optimization of LDPC codes was mostly based on the highest code rate and the best waterfall characteristics [33]. With the deepening of the research on LDPC codes, certain scholars have proposed to optimize the LDPC codes with the goal of reducing the bit error floor. Reference [34] points out the bit error floor phenomenon of complex message-passing iterative algorithm. Such a phenomenon is one of the most important obstacles in the use of LDPC codes in wireless communication systems and magnetic storage devices. The effectiveness of the LDPC code decoder relative to the BCH code and the Hamming code decoder is proved by experimental simulation, but the LDPC code has high bit error floor. Therefore, the bit error floor of the LDPC code is a major bottleneck in the development of the LDPC code. Protograph LDPC codes have similar problems. Reference [35] proposes a new system construction optimized protograph LDPC code with good decoding threshold and low bit error floor. The simulation results show that the code exhibits excellent performance in the bit error floor and the waterfall area on the additive white Gaussian noise channel. The above documents show that solving the bit error floor problem of the LDPC code can effectively improve the performance of the LDPC code. However, doing a joint optimization of code word considering waterfall and error floor characteristics is necessary due to the bad channel conditions such as severe fading and impulse noise and the unrecognizable code of the irregular LDPC code itself.

In summary, the present study will start with the parallel communication part of power line wireless dual-media cooperative communication and analyze the distribution of different fading and noise in the power line-wireless hybrid channel. The innovative work of the thesis includes the following aspects:

1) The information combination and its initial LLR calculation method in dual media parallel communication are studied based on mixed fading and impulse noise in power line and wireless parallel communication. The expectation maximization (EM) algorithm is used to estimate the parameters of PDF of the LLR after the combination. In addition, the key parameters such as weight, mean, and variance of the multi-dimensional mixed Gaussian distribution are obtained. Different from the EXIT algorithm in the traditional AWGN channel, the mean and variance of the Gaussian distribution of each dimension of the LLR after EM estimation no longer satisfy the relationship that the variance is twice the mean.
2) For the problem that the variance of GM is no longer twice of the mean, a multi-dimensional EXIT algorithm based on the Gaussian mixture model is proposed. The key function in the traditional EXIT algorithm is extended and the mutual information calculation formula of the check node derived. The Gaussian Hermit formula is used to process the approximate closed expression. Compared with the traditional algorithms, the simulation proves that the proposed expression is more suitable for power line-wireless dual media parallel cooperative communication. A multidimensional EXIT theory is proposed to evaluate the convergence performance of LDPC codes in a dual media cooperative communication system based on $J'(\sigma)$.
3) An LDPC code optimization algorithm for hybrid fading and impulse noise channels is proposed based on the multi-dimensional EXIT theory. This algorithm proves the equivalence between the overall convergence of multidimensional EXIT charts and the convergence of the whole combining EXIT ploy line chart. The problem of decoding symmetry when no double

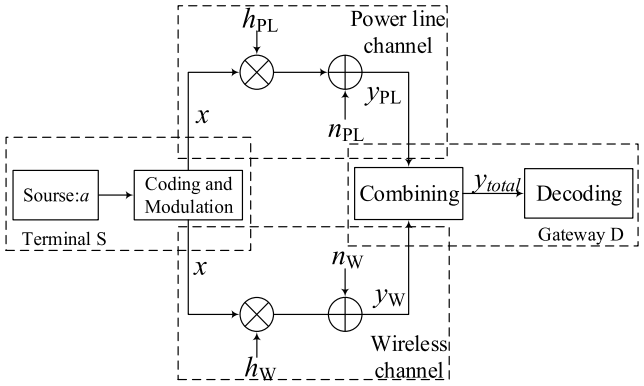

FIGURE 1. Theoretical system block diagram of power line and wireless dual-media cooperation.

relationship exists between the variance and mean of the system's LLR distribution is analyzed and verified. Gaussian Hammett and integral transform are used to derive and give the stability conditions of the LDPC code. The degree distribution of the waterfall area optimization aims at maximizing the area between the VND and CND curves based on the stability condition. After that, using the multi-dimensional EXIT chart, the approximate minimum signal-to-noise ratio (SNR) when the degree distribution is converged can be obtained. Finally, the optimization is carried out with the minimum theoretical BER as the goal. Moreover, the codeword distribution of the characteristics of the waterfall area and the bit error floor characteristics is constructed. The BER curve is also used to verify that the waterfall characteristics of the optimized degree distribution and the bit error floor are indeed better than other degrees. Then, the BER iterative graph in the iterative process is drawn to visually see the change of the BER of each round of iteration using the mutual information of each iteration of decoding. Finally, the BER iterative graph is combined with the EXIT chart to construct a three-dimensional error rate surface map, which intuitively observes the LDPC code error rate change during the iterative process.

II. SYSTEM MODEL AND PRELIMINARIES

Reference [36] shows a typical scenario of power line wireless dual media cooperation, the system model can be simplified by only considering the power line wireless parallel communication between the mobile terminal S and the gateway D without passing through the relay node. In the above model, the mobile terminal S transmits the same source a to the gateway D through the power line and the wireless channels, respectively. After LDPC encoding and BPSK modulation, source a is recorded as x. The system model is shown in Fig.1.

h_W is the wireless channel fading coefficient, which satisfies the Nakagami-m distribution. n_W is Gaussian white noise, which satisfies the normal distribution, that is $n_W \sim N\left(0, \sigma_W^2\right)$. h_{PL} is the power line channel fading coefficient which satisfies the log-normal distribution and n_{PL} is the noise of the power line channel. The messages received by the gateway D from the power line and the wireless channel are y_{PL} and y_W, respectively. Then, y_{PL} and y_W can be expressed as:

$$y_{PL} = h_{PL}x + n_{PL}, \tag{1}$$

$$y_W = h_W x + n_W. \tag{2}$$

Referring to [2], the power line channel noise is divided into background noise and impulse noise, which are independent of each other and have a Gaussian distribution that satisfies the superposition characteristics of Gaussian noise. The Bernoulli–Gaussian model is used for modeling for the impulse noise. Therefore, the additive noise of the power line channel in (1) can be split into background noise and impulse noise:

$$n_{PL} = n_{PL,B} + W_B \times n_{PL,I}, \tag{3}$$

where $n_{PL,B}$ is the power line channel background noise and $n_{PL,I}$ is the power line channel impulse noise, the variances of which are $\sigma_{PL,B}^2$ and $\sigma_{PL,I}^2$, respectively. W_B is a statistically independent and identically distributed sequence of Bernoulli random variables and the probability distribution satisfies $P\{W_B = 0\} = 1 - p$ and $P\{W_B = 1\} = p$. The probability that no impulse noise occurs in the power line channel is equal to $1 - p$ and the probability of occurrence of impulse noise is p. When the power line channel has impulse noise, the power of noise is $\sigma_{PL,I}^2$. When the power line channel has no impulse noise, the power of noise is $\sigma_{PL,B}^2$. To simplify the noise model $K = \sigma_{PL,I}^2/\sigma_{PL,B}^2$ denotes the ratio of impulse noise power to background noise power. When impulse noise exists, the power line channel power of noise is $\sigma_{PL}^2 = K \times \sigma_{PL,B}^2$.

After receiving the y_{PL} and y_W, gateway D needs to combine them to obtain the diversity gain. Common processing methods include MRC, SC, and direct combining (DC). Performance is better than alternative methods, such as selective combining because MRC can make full use of the channel's effective information [37]. Therefore, this study uses the MRC to process the signals of the dual media parallel channel. In the receiving terminal, the gateway D uses the MRC to combine the two branch signals and the combining coefficient of each branch is proportional to the channel fading and inversely proportional to the total noise power. The noise model of the power line channel includes two parts, background and impulse noises. Hence, this model is divided into two cases for analysis.

When there is only background in the sampling moment, the received signal can be expressed as:

$$y_{Total,1} = \frac{h_W}{\sigma_W^2} y_W + \frac{h_{PL}}{\sigma_{PL,B}^2} y_{PL}. \tag{4}$$

Similarly, when impulse noise exists at the sampling moment, the received signal can be calculated as:

$$y_{Total,2} = \frac{h_W}{\sigma_W^2} y_W + \frac{h_{PL}}{K \times \sigma_{PL,B}^2} y_{PL}. \tag{5}$$

where $y_{Total,1}$ indicates the result of the MRC with the wireless channel when only background noise exists in the PLC channel and $y_{Total,2}$ indicates that of the MRC with the wireless channel when background noise coexists with impulse noise in the PLC channel.

Eqs. (1) and (2) are substituted into (4):

$$y_{Total,1} = \left(\frac{h_W^2}{\sigma_W^2} + \frac{h_{PL}^2}{\sigma_{PL,B}^2}\right) x + \frac{h_W}{\sigma_W^2} n_W + \frac{h_{PL}}{\sigma_{PL,B}^2} n_{PL}, \quad (6)$$

where the power of noise in $y_{Total,1}$ is $\frac{h_W^2}{\sigma_W^2} + \frac{h_{PL}^2}{\sigma_{PL,B}^2}$.

Similarly,

$$y_{Total,2} = \left(\frac{h_W^2}{\sigma_W^2} + \frac{h_{PL}^2}{K \times \sigma_{PL,B}^2}\right) x + \frac{h_W}{\sigma_W^2} n_W + \frac{h_{PL}}{K \times \sigma_{PL,B}^2} n_{PL}, \quad (7)$$

where the power of noise in $y_{Total,2}$ is $\frac{h_W^2}{\sigma_W^2} + \frac{h_{PL}^2}{K \times \sigma_{PL,B}^2}$.

The initial LLRs corresponding to $y_{Total,1}$ and $y_{Total,2}$ are recorded as L_1 and L_2, respectively. Then, they can be computed as

$$L_1 = \frac{2\left(\frac{h_W^2}{\sigma_W^2} + \frac{h_{PL}^2}{\sigma_{PL,B}^2}\right) y_{Total,1}}{\frac{h_W^2}{\sigma_W^2} + \frac{h_{PL}^2}{\sigma_{PL,B}^2}} = 2y_{Total,1}, \quad (8)$$

$$L_2 = \frac{2\left(\frac{h_W^2}{\sigma_W^2} + \frac{h_{PL}^2}{K \times \sigma_{PL,B}^2}\right) y_{Total,2}}{\frac{h_W^2}{\sigma_W^2} + \frac{h_{PL}^2}{K \times \sigma_{PL,B}^2}} = 2y_{Total,2}, \quad (9)$$

After the receiving terminal R receives the messages transmitted from the power line and the wireless channel, the initial LLR processed by the MRC algorithm can be calculated as:

$$L_{MRC} = (1-p)\, L_1 + pL_2. \quad (10)$$

III. IMPROVED MULTIDIMENSIONAL EXIT ALGORITHM BASED ON EM ESTIMATION

The traditional EXIT chart tracks the convergence of the decoder by observing the information between the sub-decoders of the concatenated code [24]. The mutual information between the random variable X sent by the sender and the LLR L of the message received by the receiver can be calculated as

$$I(X, L) = 1 - \int_{-\infty}^{+\infty} \frac{1}{\sqrt{2\pi\sigma^2}} e^{-\frac{(l \mp \sigma^2/2)}{2\sigma^2}} \times \log_2\left(1 + e^{-l}\right) dl = J(\sigma), \quad (11)$$

where σ^2 is the noise power of the channel and the $J(\sigma)$ function is an important formula used by the traditional EXIT to calculate mutual information. On the contrary, traditional EXIT algorithm and $J(\sigma)$ are mainly used for the AWGN channel. However, the above formula is no longer applicable in the condition of power line-wireless parallel communication mixed fading and impulse noise channel. Therefore, the traditional mutual information calculation formula $J(\sigma)$ needs to be improved for the iterative decoding analysis under mixed fading and impulse noise conditions.

TABLE 1. Parameters of the Gaussian mixture.

SNR	Dimension	Mean	Variance	Weight
6dB	1	15.7010	14.5914	0.1771
	2	8.5497	6.8968	0.3450
	3	3.0410	6.0070	0.4203
	4	22.9684	133.3648	0.0576

A. AN IMPROVED EXIT ALGORITHM BASED ON EM ESTIMATION

The initialized LLR after combining includes different forms of fading from the power line and wireless channels, and the power line channel with impulse noise. Therefore, the expression of the PDF of LLR is difficult to obtain. We refer to [28]–[32] which use GMM and EM algorithm to solve this problem. After decomposition, the parameters such as mean, variance, and weight of each Gaussian component need to be estimated by the EM algorithm.

In the traditional EXIT algorithm, only the Gaussian white noise of the AWGN channel is considered. L_{BP} is the initializing LLR of BP decoding, whose distribution satisfies $L_{BP} \sim N\left(\frac{\sigma^2}{2}, \sigma^2\right)$ [25]. However, parallel communication involves mixed fading and different types of noise; hence, the PDF of the initializing LLR of BP decoding is difficult to express. Therefore, the EM algorithm is used to estimate the parameters of GM of the decoded initializing LLR so that the key parameters such as weight, mean, and variance of the initializing LLR can be obtained.

We set the following: $SNR = 6$dB, $p = 0.01$, $K = 10$, the fading parameter of Lognormal distribution in power line channel is 1.8 dB, and the parameter of Nakagami-m fading in wireless channel is $m = 1.2$. Then, the multidimensional parameters shown in Table 1 are obtained by EM estimation. Substituting these parameters into the Gaussian mixture model, the PDF of the initializing LLR can be expressed as:

$$f_L(l) = \sum_{q=1}^{Q} \frac{\omega_q}{\sqrt{2\pi\sigma_q^2}} \exp\left(-\frac{(l-\mu_q)^2}{2\sigma_q^2}\right), \quad (12)$$

where Q is the number of GM components, ω_q is the weight of the q-th dimension GM component, σ_q^2 is the variance of the q-th dimension GM component, and μ_q is the mean of the q-th dimension GM component.

The PDF of the LLR after GM is compared with the distribution of the actual LLR. Fig. 2 shows the results.

In Fig. 2, the solid black line indicates the PDF of the LLR after GM, the red dotted line indicates the distribution of the actual LLR, and the purple dash-dotted line indicates the PDF corresponding to each Gaussian component participating in the GM. Fig. 2 shows that the mixed Gaussian curve obtained by EM estimation fits well with the PDF curve of the initializing LLR of BP decoding.

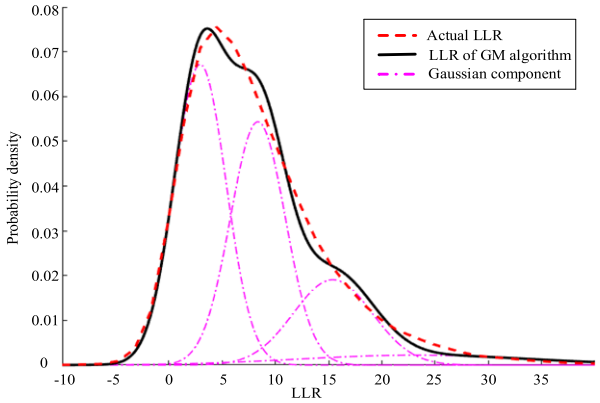

FIGURE 2. The LLR of GM algorithm estimated by EM algorithm, the components of Gaussian mixture and the actual LLR.

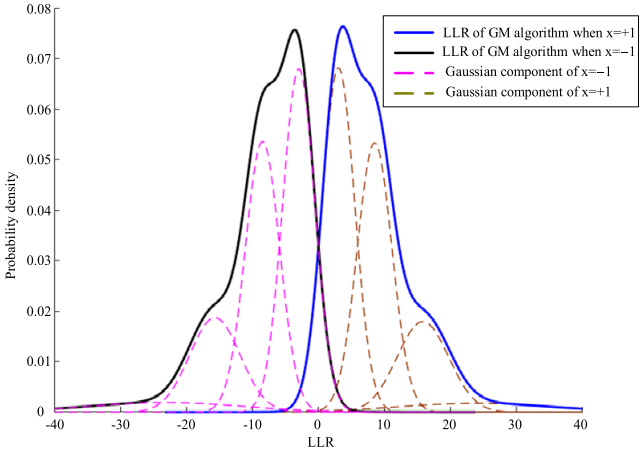

FIGURE 3. Comparison in PDF of LLR and the components of GM algorithm when the terminal S sends x = 1 and x = −1.

We also tested the symmetry of the system. First, the fading parameter of the power line channel was set as 1.5dB, $K = 10$, and $p = 0.01$. Then terminal S sends $X = +1$ for 1,000,000 times, so we can acquire 1,000,000 initializing LLR values after the MRC at terminal R. The initial LLR distribution of the terminal R is fitted by GM, and the mean, variance, and weight of the Gaussian components of each dimension are obtained by the EM algorithm. Then, the terminal S sends $X = -1$ for 1,000,000 times and repeat the above steps. Hence, we can determine the curve of PDF when sending $X = +1$ and $X = -1$.

In Fig. 3, the blue curve represents the PDF curve when $X = +1$ is sent from terminal S and the black curve is the PDF curve when $X = -1$. Table 2 shows the parameters of GM obtained by the EM algorithm. Fig. 3 clearly shows that when terminal S transmits $X = +1$ and $X = -1$, the distributions of LLR after MRC are approximately symmetric.

Table 2 shows that the parameters obtained by the EM algorithm satisfy the relationship that the means are approximately opposite to one another and the variances are approximately equal. Due to the number of Monte Carlo simulations used in the simulation is not infinite and the EM algorithm

TABLE 2. Parameters of multidimensional EXIT.

	Para.	1st	2nd	3rd	4th
$X=+1$	ω	0.35682	0.38818	0.18999	0.06501
	σ^2	6.1761	5.9643	12.732	119.39
	μ	8.2073	3.0384	14.888	21.145
$X=-1$	ω	0.35657	0.38840	0.19004	0.06499
	σ^2	6.1166	5.8656	12.501	117.35
	μ	−8.2078	−3.0082	−14.781	−21.039

itself is an approximate estimation algorithm, subtle differences are observed in the parameters such as the mean, variance, and weight. However, in total, the system can be considered to satisfy the symmetry condition. Terminal S can transmit all "0" code because the system satisfies the symmetry condition and after BPSK modulation, x is an all "+1" vector.

B. MULTIDIMENSIONAL EXIT ALGORITHM BASED ON EM ESTIMATION

Table 1 and Table 2 show that the mean and variance of each dimension no longer satisfy the relationship that the variance is twice that of the mean. In the traditional EXIT algorithm, the mutual information calculation method that the variance is twice of the mean is no longer applicable. Therefore, for the iterative decoding analysis with mixed fading and impulse noise, the traditional function needs to be improved. The objective is to calculate correctly the mutual information between the message random variable x and the q-th dimensional Gaussian component of the LLR.

After derivation, the improved mutual information calculation formula is as follows:

$$\begin{aligned} I_{X,L_q} &= 1 - \int_{-\infty}^{\infty} \frac{1}{\sqrt{2\pi\sigma_q^2}} \exp\left[-\frac{(l-\mu_q)^2}{\sigma_q^2}\right] \\ &\quad \times \log_2\left(1+\exp\left(-\frac{2\mu_q l}{\sigma_q^2}\right)\right) dl. \\ &= J'\left(\mu_q, \sigma_q\right) \end{aligned} \tag{13}$$

The derivation process is discussed in Appendix A.

When $\sigma_q^2 = 2\mu_q$, the formula degenerates to $J(\sigma) = 1 - \int_{-\infty}^{+\infty} p_L(l|+1) \cdot \log_2\left[\exp(-l)\right] dl$, which is consistent with the calculation formula in the traditional EXIT algorithm [22].

The mutual information $I(X; L)$ between the random variable X and the overall BP decoding initialization LLR can be obtained by adding the mutual information $I_{X,q}$ between random variable X and the LLR of the Gaussian components

by weights:

$$I(X;L) = \sum_{q=1}^{Q} \omega_i \left[1 - \int_{-\infty}^{+\infty} \left(\frac{\exp\left(-\frac{(l-\mu_q)^2}{2\sigma_q^2} \right)}{\sqrt{2\pi\sigma_q^2}} \times \log_2 \left(1 + \exp\left(-\frac{2\mu_q l}{\sigma_q^2} \right) \right) \right] dl = \sum_{q=1}^{N} \omega_q J'\left(\mu_q, \sigma_q\right). \quad (14)$$

In (13), $J'\left(\mu_q, \sigma_q\right)$ can be simplified by Gauss–Hermit quadrature formula to obtain an approximate numerical solution.

$$J'(\mu_q, \sigma_q) = 1 - \frac{1}{\sqrt{\pi}} \times \sum_{m=1}^{M} (c_m \times \log_2 \left[1 + \exp\left(\frac{-2\mu_q}{\sigma_q^2} \times \left(\sqrt{2} a_m \sigma_q + \mu_q \right) \right) \right]), \quad (15)$$

where c_m and a_m represent the weight and abscissa zero, respectively, and M is the Hermit integral order.

The certification process is detailed in Appendix B.

Using (14), the mutual information of the iterative decoding can be calculated according to the LLR parameters: mean, variance, and weight of the information received by the sub decoder I_E, I_A.

The process of iterative decoding has the following steps:

1) INITIALIZATION

The information of the variable node is from the adjacent check node and channel information, and the information sent by the variable node to the i-th check node can be calculated as:

$$L_{i,out} = L_{ch} + \sum_{i \neq j} L_{j,in}, \quad (16)$$

where L_{ch} represents channel information and $L_{j,in}$ is information transmitted by the j-th check node. The information sent by the check node is assumed to satisfy approximately the Gaussian distribution. Then, the above formula in the form of Gaussian distribution summation and the LLR output by the variable node is in the form of a mixed Gaussian distribution. Hence, the mean and the variance respectively satisfy with:

$$\mu_{vc,q}^{(l)} = (k-1)\,\mu_{cv,q}^{(l-1)} + \mu_{ch,q}, \quad (17)$$

$$\sigma_{vc,q}^{2\ (l)} = (k-1)\,\sigma_{cv,q}^{2\ (l-1)} + \sigma_{ch,q}^2, \quad (18)$$

where q corresponds to the q-th Gaussian component ($q = 1, \ldots, Q$) in the mixed Gaussian distribution, l represents the l-th iteration, k is the degree of the variable node, subscript vc represents the variable node to the check node, subscript cv represents the check node to the variable node, and $\mu_{ch,q}$ and $\sigma_{ch,q}^2$ are the mean and variance of the q-th Gaussian component estimated by the EM algorithm. When the number of iterations $l = 1$, the previous iteration information $\mu_{cv,q}^{(0)} = 0$, $\sigma_{cv,q}^{2\ (0)} = 0$.

2) FROM THE VARIABLE NODE TO CHECK NODE

In the l-th round iteration, the output information of the mixed Gaussian component of the q-th dimension of the variable node is

$$I_{vc,q}^{l}\left(\lambda_k, \mu_{vc,q}^{(l)}, \sigma_{vc,q}^{2\ (l)}\right) = \sum_{k=2}^{d_v} \lambda_k J'\left(\mu_{vc,q}^{(l)}, \sigma_{vc,q}^{2\ (l)}\right), \quad (19)$$

where λ_k represents the proportion of edges connected to the variable node of degree k.

The output information of each dimension Gaussian component at the variable node is obtained by (19). Hence, the total output information of the variable node is

$$I_{vc}^{l}\left(\lambda_k, \mu_{vc,q}^{(l)}, \sigma_{vc,q}^{(l)}\right) = \sum_{q=1}^{Q} \omega_q I_{vc,q}^{l} = \sum_{q=1}^{Q} \omega_q \left[\sum_{k=2}^{d_v} \lambda_k J'\left(\mu_{vc,q}^{(l)}, \sigma_{vc,q}^{(l)}\right) \right]. \quad (20)$$

3) FROM THE CHECK NODE TO VARIABLE NODE

No linear equation expression is observed between the output information $L_{cv}^{(l)}$ of the check node and the input information of check nodes $L_{vc}^{(l)}$ from the neighboring variable nodes. For the sake of simple calculation, the LLR of the check node receiving from the variable node is assumed to satisfy approximately the gaussian distribution of $N\left(\mu_{cv}, 2\mu_{cv}\right)$, so that

$$I_{cv,q,j}^{(l)}\left(\lambda_k, \rho_j, \mu_{vc,q}^{(l)}, \sigma_{vc,q}^{(l)}\right) = 1 - J\left(\sqrt{j-1} \cdot J^{-1}\left(1 - I_{vc,q}^{l}\right)\right). \quad (21)$$

The check node degrees are not unique to meet the code rate requirements. Generally, a continuous positive integer is denoted as d_c, d_c-1, …, d_c-s,Where d_c represents the largest number of degree of check nodes. The proportions of the edges connected to them are ρ_{d_c}, ρ_{d_c-1}, …, ρ_{d_c-s}, respectively. Then, in the *l-th* round of iteration, the component output information of the q-th GM of the check node can be calculated as:

$$I_{cv,q}^{(l)}\left(\lambda_k, \rho_j, \mu_{vc,q}^{(l)}, \sigma_{vc,q}^{(l)}\right) = \sum_{j=d_c-s}^{d_c} I_{cv,q,j}^{(l)} = \sum_{j=d_c-s}^{d_c} \rho_j \left[1 - J\left(\sqrt{j-1} \cdot J^{-1}\left(1 - I_{vc,q}^{l}\right)\right) \right], \quad (22)$$

So that the l-th iteration output information of check node I_{cv} can be calculated as:

$$I_{cv}^{(l)} = \sum_{q=1}^{Q} \omega_q \times I_{cv,q}^{(l)}, \tag{23}$$

According to the output information of each dimension of the Gaussian component at the check node, the variance and mean of the check node output information LLR are expressed respectively as:

$$\sigma_{cv,q}^{2\ (l)} = \left(J^{-1}\left(I_{cv,q}^{(l)}\right)\right)^2, \tag{24}$$

$$\mu_{cv,q}^{(l)} = \frac{\sigma_{cv,q}^{2\ (l)}}{2} = \frac{\left(J^{-1}\left(I_{cv,q}^{(l)}\right)\right)^2}{2}. \tag{25}$$

Notably, the traditional method is still used, that is, $J^{-1}(\cdot)$ is used to calculate the variance and mean of the Gaussian distribution of each dimension that the check node passes to the variable node. However, (17) and (18) show the total variance in the next round is not twice the mean because the variance of the initialization channel LLR is still not twice the mean. It is necessary to calculate the mutual information by using (13)-(14). After that, the check node outputs LLR information to the variable node to start a new round of iteration. For the new round l, the last round is recorded as $l-1$ and $\mu_{cv,q}^{(l-1)}$ and $\sigma_{cv,q}^{2\ (l-1)}$ are substituted into (17) and (18). Then, a new round of iteration information will be calculated.

4) CONVERGENCE JUDGMENT

After multiple rounds of information iteration, the final mutual information no longer changes. If the output mutual information of the variable node and the check node are both 1 in the final, the iterative decoding of the degree distribution is considered successful, and vice versa.

EXIT analysis can be performed according to the above iterative decoding process. The output mutual information of the variable and check nodes are recorded as y and x, respectively, and they are drawn in the same coordinate system to obtain an EXIT chart based on the EM estimation.

Taking the (3,6) code as an example, in the first iteration, the EM estimation parameters in Table 1 are substituted into (19) and the outputs of each dimension Gaussian mixture component are:

$$I_{vc,1}^{0} = 0.9119, I_{vc,2}^{0} = 0.9993,$$
$$I_{vc,3}^{0} = 0.9978, I_{vc,4}^{0} = 0.6263.$$

Substituting $I_{vc,q}^{0}$ $(q = 1, 2, 3, 4)$ into (20) can obtain that

$$I_{vc}^{0} = \sum_{q=1}^{4} \omega_q I_{vc,q}^{0} = 0.8382.$$

The check node does not transmit information during initialization, so $I_{cv}^{0} = 0$. For the sake of convenience in simulation, we will record I_{cv}^{0} as 0.0001. Then, the coordinates of the first point in Fig. 4 are (0.0001,0.8382). When calculating the mutual information of the check node, substituting $I_{vc,q}^{1}, j = 6$, and $\rho_6 = 1$ into (22) results in:

$$I_{cv,1}^{1} = 0.6428, I_{cv,2}^{1} = 0.9955,$$
$$I_{cv,3}^{1} = 0.9897, I_{vc,4}^{1} = 0.1204.$$

Then, $I_{cv,q}^{1}$ $(q = 1, 2, 3, 4)$ is substituted into (23) and it can obtain that

$$I_{cv}^{1} = \sum_{q=1}^{4} \omega_q I_{cv,q}^{1} = 0.6083.$$

Therefore, the coordinates of the second point in Fig. 4 are (0.6083, 0.8382). Finally, the mean and variance of the output information of the check node are substituted into (17) and (18) to start the next iteration. Similarly, the coordinates of the third point can be calculated as (0.6083, 0.8866).

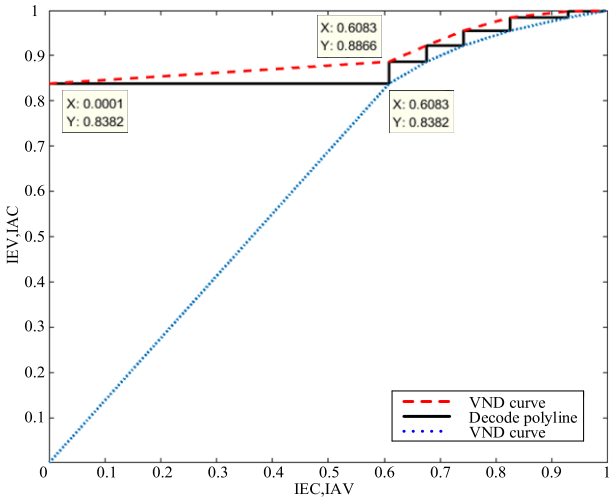

FIGURE 4. EXIT polyline chart of (3, 6) code with SNR of 6 dB.

The decoding is successful when the polyline finally converges to 1. At this point, the VND curve must always be above the CND curve. Otherwise, the decoding is unsuccessful. Given that we use the mutual information output of each dimension when calculating the iterative mutual information, we can also perform EXIT analysis on each dimension and draw a multidimensional EXIT chart. The relationship between each dimension variable node and the check node output mutual information can be obtained as follows:

$$I_{vc,q}\left(\lambda_k, I_{cv,q}\right) = \sum_{k=2}^{d_v} \lambda_k J'\left(\frac{(k-1)}{2}\left(J^{-1}\left(I_{cv,q}\right)\right)^2 + \mu_{ch,q}, (k-1)\left(J^{-1}\left(I_{cv,q}\right)\right)^2 + \sigma_{ch,q}^2\right). \tag{26}$$

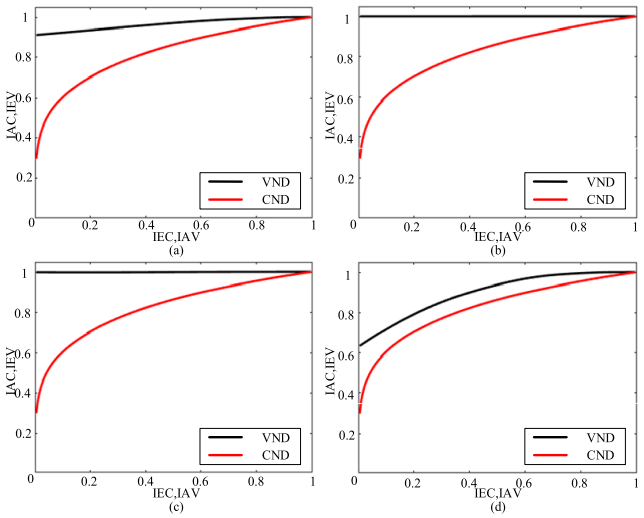

FIGURE 5. Multi-dimensional EXIT chart of the (3,6) code with a signal to noise ratio of 6 dB.

$$I_{cv,q}(\rho_j, I_{vc,q}) = \sum_{j=d_c-s}^{d_c} I_{cv,q,j} = \sum_{j=d_c-s}^{d_c} \rho_j \left[1 - J\left(\sqrt{j-1} \cdot J^{-1}\left(1 - I_{vc,q}\right)\right)\right]. \tag{27}$$

When λ_k and ρ_j are determined, the above equation can be regarded as the $I_{cv,q}\left(I_{vc,q}\right)$ function of the q-th Gaussian mixture component that produces mutual information $I_{vc,q}$ at the variable node and the $I_{vc,q}\left(I_{cv,q}\right)$ function of the mutual information output, $I_{cv,q}$ of the check node. By taking the independent variables of the two functions uniformly, the mutual information output curve VND of the variable node and the mutual information output curve CND of the q-th dimension of the check node can be obtained. Then, the two curves obtained are drawn in the same coordinate axis to obtain a multidimensional EXIT chart. Fig. 5 presents the multidimensional EXIT chart of the (3,6) code with $Q = 4$.

The black curve in Fig. 5 is the VND curve and the red curve is the CND curve. If the VND curve for each dimension is always above the CND curve, then the decoding is successful.

Unlike the traditional EXIT, which can only be analyzed iteratively for the one-dimensional parameters in the AWGN channel, the improved EXIT algorithm based on the EM estimation can analyze iteratively the multi-dimensional mean and variance parameters in the wireless power line. Moreover, in the real channel, the variance is often not twice the mean and the EXIT algorithm based on the EM estimation can overcome the limitation of the parameter problem. The decoding fails if any dimension of the multidimensional EXIT chart does not satisfy the VND curve above the CND curve. The performance in the EXIT polyline chart cannot converge to 1. We derive the relationship between the EXIT polyline chart and the multidimensional EXIT chart in next part.

In summary, the improved EXIT algorithm has strong versatility and portability. We can use the characteristics of the multidimensional EXIT and EXIT polyline charts to construct and optimize the LDPC code.

C. BER CALCULATION OF MULTIDIMENSIONAL EXIT CHART

According to the multi-dimensional EXIT theory described above and the BER calculation formula under the traditional EXIT provided in [22], we derive the theoretical BER calculation formula under the multi-dimensional EXIT as follows:

$$BER^{(l)} = \frac{1}{2}\sum_{q=1}^{Q} \omega_q erfc\left(\frac{1}{2\sqrt{2}} \times \sqrt{\sigma_{ch,q}^2 + \left(J^{-1}\left(I_{vc,q}^{(l)}\right)\right)^2 + \left(J^{-1}\left(I_{cv,q}^{(l)}\right)\right)^2}\right), \tag{28}$$

where $I_{cv,q}^{l}$ denotes the output mutual information of the q-th mixed Gaussian component in the l-th iteration and $\left(J^{-1}\left(I_{vc,q}^{(l)}\right)\right)^2$ denotes the variance of the variable node (LLR) of the q-th mixed Gaussian component in the l-th iteration, that is, $\sigma_{vc,q}^{2\ (l)}$, which can be calculated by (18). The equation above can not only be used to analyze the BER when stopping the iteration but also to calculate the BER in the current state according to the mutual information values of the two decoders in the iterative process, which is convenient for analyzing the progressive performance of the LDPC code error rate during iterative decoding.

IV. OPTIMIZATION OF LDPC CODE DISTRIBUTION BASED ON MULTIDIMENSIONAL EXIT CHART

In this section, an optimality distribution is constructed for a parallel communication system with mixed fading and impulse noise. First, the stability conditions of the LDPC codes in mixed fading conditions are derived. Then, the constraints of code convergence are provided by demonstrating the equivalence relation between the entire combining EXIT polyline chart and the multi-dimensional EXIT chart convergence. Finally, the problem of LDPC code degree distribution optimization is abstracted as the problem of finding the maximum value in the continuous space nonlinear cost equation, which can be solved by differential optimization:

1) Firstly, the maximum area between the curves is optimized and the degree distribution that maximizes the area between the curves constructed.
2) Then, on the basis of the optimal distribution of the waterfall area and the EM estimation parameters, we use the iterative convergence results of the multi-dimensional EXIT chart to obtain the minimum SNR (which we call the quasi-noise threshold) required for code convergence.
3) Finally, at the quasi-noise threshold, the minimum BER in the l-th iteration is optimized to construct the optimal distribution of the performance of the bit error floor.

A. CONSTRAINTS

1) STABILITY CONDITIONS

The BP decoding algorithm requires a symmetric and stable channel output signal. If the channel output signal is symmetric and stable, the BP decoding algorithm can make the decoding error probability arbitrarily small; otherwise, the decoding error probability must be greater than a certain value.

The stability condition of the LDPC code is $\lambda'(0)\rho'(1) < e^{s}$, where $s = -\log\left[2\int_0^{\infty} p_0(x)\, e^{-x/2} dx\right]$ and $\lambda(x)$ and $\rho(x)$ are the variable node and check node degree distributions of the LDPC code, respectively. In the AWGN channel, according to the density function of the channel initialization message LLR and the definition of the stability condition, e^{-s} can be expressed as:

$$\begin{aligned}\exp(-s) &= 2\int_0^{\infty} p_0(x)\exp\left(-\frac{x}{2}\right)dx \\ &= 2\int_0^{\infty} \frac{\sigma}{2\sqrt{2\pi}}\exp\left(-\frac{\left(x-2/\sigma^2\right)^2}{8/\sigma^2}\right)\exp\left(-\frac{x}{2}\right)dx \\ &= \exp\left(-\frac{1}{2\sigma^2}\right), \end{aligned} \tag{29}$$

where σ^2 represents the variance of the channel noise. Therefore, the stability condition of the LDPC code in AWGN channel is $\lambda'(0)\rho'(1) < \exp\left(\frac{1}{2\sigma^2}\right)$ In symmetry conditions, assuming that the channel transmits all "1" codes, then $p_0(x)$ satisfies the Gaussian distribution with a variance of twice the mean, that is, $p_0(x) \sim N\left(2/\sigma^2, 4/\sigma^2\right)$.

In the mixed fading channel, the stability condition must be reanalyzed because the variance of the LLR distribution obtained by the EM estimation is no longer twice the mean. e^{-s} can be expressed as:

$$\begin{aligned}\exp(-s) &= 2\int_0^{+\infty} p_0(x)\exp\left(-\frac{x}{2}\right)dx \\ &= \sum_{q=1}^{Q}\omega_q\left[2\times\frac{1}{\sqrt{2\pi\sigma_q^2}}\right. \\ &\quad\left.\times\int_0^{+\infty}\exp\left(-\frac{(x-\mu_q)}{2\sigma_q^2}\right)\exp\left(-\frac{x}{2}\right)dx\right]. \end{aligned} \tag{30}$$

Using the integral transformation method, the above formula can be converted into

$$\begin{aligned}\exp(-s) = \sum_{q=1}^{Q}\omega_q\left[\exp\left(\frac{\left(\sigma_q^2-4\mu_q\right)}{8}\right)\right. \\ \left.\times\left[1-\Phi\left(\frac{\sigma_q^2-2\mu_q}{2\sqrt{2}\sigma_q}\right)\right]\right], \end{aligned} \tag{31}$$

where ω_q is the weight of the q-th dimensional mixed Gaussian component, σ_q^2 is the variance of the q-th dimensional Gaussian component, μ_q is the mean of the q-th dimensional mixed Gaussian component, Q is the number of mixed Gaussian components, and Φ is the Gaussian error function.

The certification process is detailed in Appendix C.

In the mixed fading channel of parallel communication, the stability condition is

$$\begin{aligned}\lambda'(0)\rho'(1) < 1/\sum_{q=1}^{Q}\omega_q\left\{\exp\left(\frac{\left(\sigma_q^2-4\mu_q\right)}{8}\right)\right. \\ \left.\times\left[1-\Phi\left(\frac{\sigma_q^2-2\mu_q}{2\sqrt{2}\sigma_q}\right)\right]\right\}. \end{aligned} \tag{32}$$

In the AWGN channel, be substituting $\sigma_i^2 = 2\mu_i$ into (32), the following can be obtained:

$$\lambda'(0)\rho'(1) < 1/\sum_{q=1}^{Q}\omega_q\left[\exp\left(\frac{-\sigma_q^2}{8}\right)\times[1-\Phi(0)]\right]. \tag{33}$$

Given that $\Phi(0) = 0$, the simplification result is

$$\lambda'(0)\rho'(1) < 1/\sum_{q=1}^{Q}\omega_q\left[\exp\left(\frac{-\sigma_q^2}{8}\right)\right]. \tag{34}$$

By substituting $\sigma_q^2 = 4/\sigma^2$ into the simplification, the following can be obtained:

$$\lambda'(0)\rho'(1) < \sum_{q=1}^{Q}\omega_q\left[\exp\left(\frac{1}{2\sigma^2}\right)\right]. \tag{35}$$

In the AWGN channel condition, the above equation degenerates into the stability condition of the traditional EXIT algorithm. This result shows that the stability conditions in the hybrid fading channel we provide are compatible with the AWGN channel conditions.

2) CONVERGENCE JUDGMENT

The convergence of the traditional EXIT chart is based on the VND curve, which is always above the CND curve and eventually converges to 1 [27]. Figs. 4 and 5 indicate that under the mixed fading model with the modified EXIT algorithm and in both the EXIT polyline and multidimensional EXIT charts, the VND curves are always above the CND curve and eventually converge to 1. This is the convergence condition based on the modified EXIT algorithm. The following will prove that the convergence of the EXIT polyline chart and that of the multidimensional EXIT chart are mutually necessary and sufficient conditions.

Lemma: The necessary and sufficient condition for the multi-dimensional EXIT and EXIT polyline charts to converge to 1 is that the CND and the VND curves of each dimension must not intersect (they should only intersect or converge to the value 1 corresponding to (1, 1) in EXIT curve).

a: PROOF OF THE SUFFICIENCY

Iev_{q,x_t} and Iec_{q,x_t} represent the output mutual information of the variable and check node, respectively, when the abscissa is $x_t, t \in (1, 2, \ldots, T), x_t \in (0, 1)$ in the q-th dimension. For any dimension and coordinate x_t, $Iev_{q,x_t} > Iec_{q,x_t}$, that is, the VND curve of each dimension of the mixed Gaussian component in the multi-dimensional EXIT chart is above the CND curve:

$$Iev_x = \sum_{q=1}^{Q} \omega_q Iev_{q,x_q} > \sum_{q=1}^{Q} \omega_q Iec_{q,x_q} = Iec_x.$$

The equation above shows that when the VND curve of each dimension is above the CND curve in the multidimensional EXIT chart, the VND curve must be above the CND curve in the EXIT polyline chart. That is, the convergence condition of the EXIT polyline chart is satisfied.

$$Iev_x = \sum_{q=1}^{Q} \omega_q Iev_{q,x_q} > \sum_{q=1}^{Q} \omega_q Iec_{q,x_q} = Iec_x.$$

b: PROOF OF THE NECESSITY

Supposing a multidimensional EXIT chart containing Q-dimensional mixed Gaussian components can converge to 1, if one dimension does not converge, the rest converge to 1. Let the dimension that does not converge be the Q-th dimension. Then, $\forall x_t \in (0, 1)$, must have

$$\begin{cases} Iev_{1,x_t} > Iec_{1,x_t} \\ Iev_{2,x_t} > Iec_{2,x_t} \\ \cdots \\ Iev_{Q-1,x_t} > Iec_{Q-1,x_t} \end{cases},$$

and $\exists x_t \in (0, 1)$ must have $Iev_{Q,x_t} = Iec_{Q,x_t} < 1$. Then, given $\sum_{q=1}^{Q} \omega_q = 1$, the EXIT polyline chart must have

$$\begin{cases} Iev_x = \sum_{q=1}^{Q} \omega_q Iev_{q,x_t} < 1 \\ Iec_x = \sum_{q=1}^{Q} \omega_q Iec_{q,x_t} < 1 \end{cases}.$$

Thus, the EXIT polyline chart cannot converge to 1, that is, the EXIT polyline chart does not converge.

In summary, the convergence of the EXIT polyline chart and that of the multidimensional EXIT chart are mutually necessary and sufficient conditions.

B. DEGREE DISTRIBUTION OPTIMIZATION

The optimization of the degree distribution includes mainly the optimization of the waterfall area and the bit error floor area. The goal of waterfall area optimization is to quickly find the approximate noise threshold of the decoding, which considerably reduces the time spent on the bit error floor area optimization while ensuring excellent waterfall characteristics of the bit error floor area optimization results. The bit error floor area optimization aims to reduce the error floor when the decoding converges and finally construct a degree distribution with excellent performance in both the waterfall and bit error floor areas.

1) WATERFALL AREA OPTIMIZATION (WFA OPT.)

The portion between the VND and CND curves in the EXIT chart is the decoding channel of the LDPC code. The spacing between the two curves of the EXIT chart will shrink with the decrease of SNR, and eventually intersecting and resulting in failure to decode correctly.

In designing an LDPC code in a power line-wireless mixed channel suitable for unstable channel conditions, when the code rate is fixed, the optimal degree distribution should be constructed so that the area between the two curves is the largest and can withstand severe channel conditions. So it can be successfully decoded at a lower SNR. The waterfall area corresponding to the BER curve will also come earlier.

Arbitrarily select a high signal-to-noise ratio and a suitable code rate R. In each dimension of the multi-dimensional EXIT chart, uniformly take T points on the VND and CND curves, respectively denoted as Iev_{q,x_t}, Iec_{q,x_t}, where q denotes the first q-th dimensions; $t \in (1, 2, \cdots, T)$ represents the t-th point. The area of a single dimension is approximately

$$s_q = \frac{\sum_{t=1}^{T} \left(Iev_{q,x_t} - Iec_{q,x_t} \right)}{T}. \tag{36}$$

The total area of the final multidimensional EXIT chart is

$$S = \sum_{q=1}^{Q} \left(\omega_q \times s_q \right), \tag{37}$$

where Q is the total number of dimensions estimated by EM and w_q is the weight of the q-th dimension estimated by the EM algorithm.

The constraint conditions are the stability and convergence conditions of the LDPC code in the mixed fading channel. These two constraints are the premise that the codeword can be decoded correctly. The total area ($S = 0$) is considered if the code word does not satisfy the stability or convergence condition.

In summary, the code word waterfall area performs better and can withstand more severe channel conditions when the total area (S) is the largest.

$$\begin{aligned} &\text{Maximize}: S = \sum_{q=1}^{Q} \left(\omega_q \times s_q \right), \\ &\text{Subject to}: \lambda'(0)\, \rho'(1) < 1 / \sum_{q=1}^{Q} \omega_q \left[\exp\left(\frac{\left(\sigma_q^2 - 4\mu_q \right)}{8} \right) \right. \\ &\qquad \left. \times \left[1 - \Phi\left(\frac{\sigma_q^2 - 2\mu_q}{2\sqrt{2}\sigma_q} \right) \right] \right], \\ &Iev_{q,x_t}\left(\lambda, \mu_q, \sigma_q^2 \right) > Iec_{q,x_t}\left(\rho, \mu_q, \sigma_q^2 \right) \\ &\qquad \left(q \in [1, 2, 3, \cdots, Q], t \in [1, 2, 3, \cdots, T] \right). \end{aligned}$$

Taking the maximum area between the curves as the target and satisfying the stability and convergence conditions as constraint conditions for differential evolution, the degree distribution of the waterfall area with excellent performance can be obtained. The SNR corresponding to the waterfall area can be obtained by calculating the BER of the degree distribution. The SNR can be approximated as the noise threshold that the channel can be decoded correctly, that is, the quasi-noise threshold. The EM estimation must be repeated for different SNRs when performing BER simulation. The simplification method determines the quasi-noise threshold by performing several tests on the SNR using the dichotomy.

2) ERROR FLOOR AREA OPTIMIZATION (EFA OPT.)

After the optimization in the waterfall area, the quasi-noise threshold is obtained and the bit error floor is optimized under a quasi-noise threshold to obtain a distribution of excellent waterfall and bit error floor characteristics. The BER of the degree distribution can be obtained by (28), the minimum BER at the final convergence is optimized for the optimization target and the bit error floor area of the optimized distribution is improved.

$$\begin{aligned}
&\text{Minimize } BER = \frac{1}{2}\sum_{q=1}^{Q}\omega_q \\
&\quad \times erfc\left(\frac{\sqrt{\sigma_{ch,q}^2 + \left(J^{-1}\left(I_{vc,q}\right)\right)^2 + \left(J^{-1}\left(I_{cv,q}\right)\right)^2}}{2\sqrt{2}}\right), \\
&\text{Subject to: } \lambda'(0)\,\rho'(1) < 1/\sum_{q=1}^{Q}\omega_q\left[\exp\left(\frac{\left(\sigma_q^2 - 4\mu_q\right)}{8}\right)\right. \\
&\quad \left.\times\left[1 - \Phi\left(\frac{\sigma_q^2 - 2\mu_q}{2\sqrt{2}\sigma_q}\right)\right]\right], \\
&\quad Iev_{q,x_t}\left(\lambda, \mu_q, \sigma_q^2\right) > Iec_{i,x_t}\left(\rho, \mu_q, \sigma_q^2\right) \\
&\quad (q \in [1, 2, 3, \cdots, Q], t \in [1, 2, 3, \cdots, T]).
\end{aligned}$$

The degree distribution with excellent performance in the waterfall area and the bit error floor can be obtained by finding the appropriate degree distribution through differential optimization.

The selection of the quasi-noise threshold is of great significance for the optimization of the bit error floor. It overcomes the difficulty of excessive optimization caused by massive search and reduces the number of differential optimizations considerably and only requires a differential evolution at the quasi-noise threshold to obtain the required optimality distribution. The quasi-noise threshold still has some optimizable space compared to the actual noise threshold. Therefore, when the quasi-noise threshold is optimized for the bit error floor, the target with the lowest BER is optimized, and the details of the EXIT curve can be adjusted. Thus, the EXIT curve not only ensures good waterfall characteristics but also satisfies the best error floor.

V. SIMULATION RESULTS

The experiment was performed using Matlab. The wireless channel fading is a Nakagami-m distribution, the noise is Gaussian white noise. The power line channel fading is a log-normal distribution, and the impulse noise is modeled by the Bernoulli–Gaussian model. Similar to [30], the fixed power line fading parameter is 1.8, the impulse to background noise power ratio K is 10, the m of Nakagami-m fading model is 1.2, and the impulse noise occurrence probability p is 0.01. Both channels are energy normalized.

The SNR is set to 6 dB and the above parameters are substituted into (8)-(10) to generate the LLR values. Gaussian mixture fitting is performed on the distribution of these initialized LLR values and the Gaussian mixing parameters are obtained by the EM algorithm. The Gaussian mixing parameters are shown in Table 1.

First, the waterfall area is optimized. Compared with common code words, such as the (3, 6) code, the degree of distribution code rate that need to be optimized is set to 0.5. After the optimization of the waterfall area, the optimal degree distribution is obtained as shown in Table 3. Based on the above degree distribution and EM estimation parameters, an improved EXIT algorithm can be used to draw an EXIT line graph, based on the above degree distribution and the EM estimation parameters as shown in Fig. 6.

Figs. 6 (a), (b) present the EXIT decoding polyline, which correspond to the degree distribution with the largest area as the optimization target and (3, 6) code, respectively. Both of them performed on a channel with an SNR of 5 dB. In Fig. 6(a) only a few iterations are required to converge while the curves in Fig. 6(b) need more iterations to converge. Figs. 6(c), (d) show the EXIT decoding polyline, which correspond to optimized degree distribution and (3, 6) code, respectively. The degree distributions performed on a channel with an SNR of 4.1 dB.

The comparison of Fig. 6 (a) with Fig. 6 (c) indicates that the decoding channel narrows and the number of iterations increases as the SNR decreases. The comparison of Fig. 6 (c) and Fig. 6 (d) show that the convergence results of different degree distributions at the same SNR will be quite different. The degree distribution obtained by optimization is significantly better than the (3, 6) code with the same code rate of 0.5.

In part IV, we demonstrate that the multidimensional EXIT chart is equivalent to the convergence condition of the EXIT polyline chart. Fig. 7 shows the multi-dimensional EXIT chart corresponding to the EXIT polyline chart of Fig. 6. The multi-dimensional EXIT charts is similar to Fig.7. We now only discuss the narrowest dimensions among them which limit the convergence.

Figs. 7(a) and (b) are simulations of WFA optimization degree distribution and (3, 6) code with an SNR of 5 dB. Figs. 7(c) and (d) are simulations of WFA optimization

TABLE 3. Degree distribution obtained through different conditions and different optimization strategies.

Channel fading and noise	Code rate	Optimization strategy	Initial SNR before optimization	Variable node degree distribution					Check node degree distribution	
				λ_2	λ_3	λ_4	λ_5	λ_{20}	ρ_{10}	ρ_{11}
				0.4640	0.3702	0.0665	0.0506	0.0487	0.5761	0.4239
	R=0.75	WFA Opt.	6.0dB	λ_2	λ_3	λ_6	λ_{11}	λ_{20}	ρ_7	ρ_8
				0.9887	0.0063	0.0018	0.0005	0.0027	0.3315	0.6685
		Joint Opt.	5.0dB	λ_2	λ_3	λ_4	λ_5	λ_{20}	ρ_{13}	ρ_{14}
P=0.01 m=1.2				0.4421	0.0519	0.1225	0.0284	0.3551	0.3204	0.6796
		EFA Opt.	6.0dB	λ_2	λ_3	λ_4	λ_5	λ_{20}	ρ_5	ρ_6
				0.3591	0.4355	0.1630	0.0180	0.0244	0.5595	0.4405
	R=0.5	WFA Opt.	6.0dB	λ_2	λ_3	λ_4	λ_5	λ_{20}	ρ_4	ρ_5
				0.9833	0.0066	0.0047	0.0041	0.0013	0.9626	0.0374
		Joint Opt.	4.1dB	λ_2	λ_3	λ_4	λ_5	λ_{20}	ρ_5	ρ_6
				0.6281	0.1083	0.0076	0.0151	0.2409	0.5119	0.4881
		WFA Opt.	6.0dB	λ_2	λ_3	λ_6	λ_{10}	λ_{20}	ρ_7	ρ_8
P=0.05 m=1.2	R=0.5			0.2139	0.2448	0.4082	0.1305	0.0026	0.6929	0.3071
		Joint Opt.	5.0dB	λ_2	λ_3	λ_4	λ_5	λ_{20}	ρ_{10}	ρ_{11}
				0.0768	0.2154	0.0850	0.2234	0.3994	0.9197	0.0803
		WFA Opt.	6.0dB	λ_2	λ_3	λ_4	λ_{12}	λ_{20}	ρ_4	ρ_5
P=0.01 m=0.6	R=0.5			0.9670	0.0139	0.0111	0.0055	0.0025	0.9458	0.0542
		Joint Opt.	4.1dB	λ_2	λ_3	λ_4	λ_5	λ_{20}	ρ_4	ρ_5
				0.6970	0.1626	0.0081	0.0030	0.1293	0.1424	0.8576

degree distribution and (3, 6) code with an SNR of 4.1 dB. The black curve represents the VND curve and the red curve represents the CND curve. The comparison of Figs. 7(a) and (b) indicate that although both of the two curves in Figs. 7(a) and (b) can converge to 1 without intersect, the curves in Fig. 7(a) have more space which can withstand worse channel conditions. From Figs. 7(c) and (d), it can be seen that the VND and CND curves of (3, 6) code intersect before (1, 1) when the SNR comes to 4.1 dB while the curves of WFA optimization degree distribution are almost tangent with each other. Comparing Figs. 7(a) and (c) and Figs. 7(b) and (d), it is concluded that the decrease of SNR can cause the decoding channel to become narrower of even turned off, which serves as our theoretical basis for finding the quasi-decoding threshold of the code by reducing the SNR gradually.

Different degree distributions with the same code rate 0.5 at different SNR are simulated. The WFA Opt. distribution, the EFA Opt. distribution, the Joint Opt. distribution, the (3,6) code, the (4,8) code and the code used in 802.11 and 802.16e wireless standards [38] are compared in terms of BER and waterfall area characteristic. The chosen LDPC codes of 802.11 and 802.16e are with the same frame length of 1944 and the same code rate of 0.5. They can be decoded by a layer BP algorithm with a limited iterations. The comparison results are shown in Fig. 8. It indicates that the degree distribution of the WFA optimization has a good waterfall area characteristic but the bit error floor characteristic is slightly poor. The EFA optimization has the best error characteristics after convergence but the waterfall characteristic is poor and similar to the (3,6) code. This finding indicates that the optimization of the WFA plays an important role in the entire optimization process. Only EFA optimization near the decoding threshold can get the best degree distribution. After the WFA optimization, it can be observed that the quasi noise threshold is 4.1 dB.

The EM estimated parameter with SNR of 4.1 dB is substituted into the differential optimization algorithm and the degree distribution obtained by optimizing the BER is the optimal degree distribution. The optimum distribution is superior to the degree distribution optimized by the WFA because the WFA optimization aims to maximize the area between curves and is used to approximate the actual decoding threshold. The optimization with the lowest BER adjusts the shape of the curve by changing the degree distribution so that the two curves fit more closely. Contrasting the Joint Opt. codes with the LDPC distribution in 802.11 and 802.16, it can be observed that the Joint Opt is better in waterfall and bit error characteristic. In summary, the degree distribution constructed by the optimization algorithm provided in this

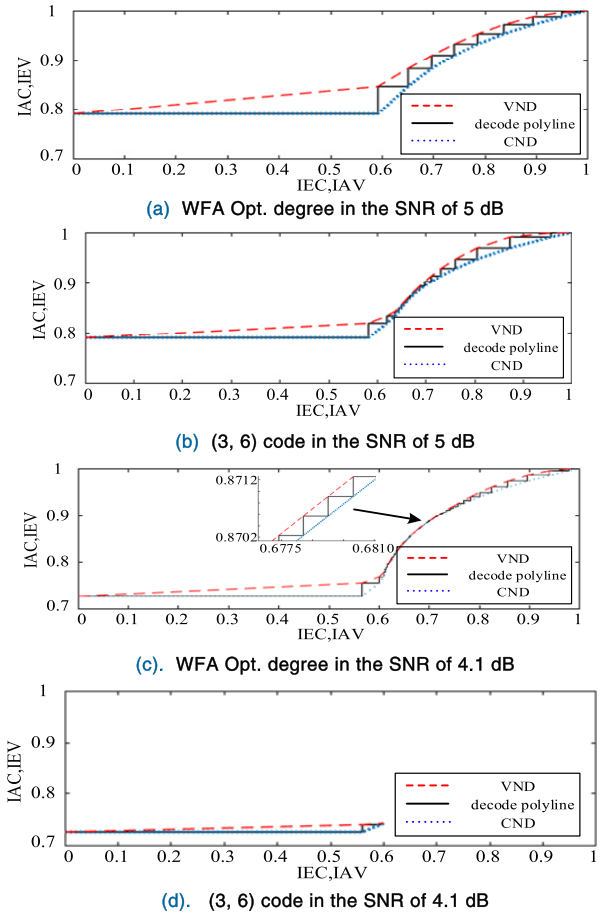

FIGURE 6. EXIT polyline charts with WFA Opt. code and (3,6) code in with different SNRs.

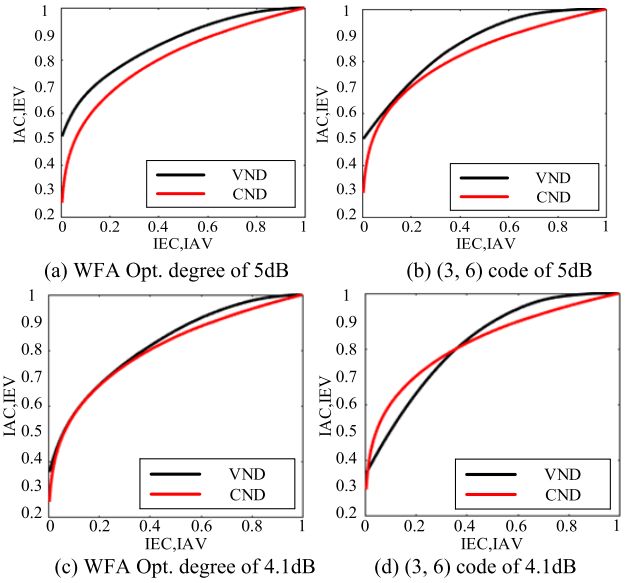

FIGURE 7. The narrowest dimension of the multi-dimensional EXIT charts.

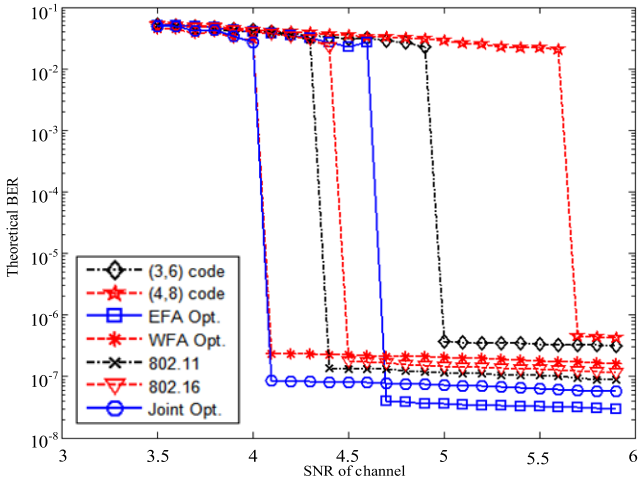

FIGURE 8. Theoretical BER graph of different codes.

paper has certain advantages in terms of the power line and wireless dual media cooperative communication system. The fading and impulse noise parameters are unchanged and the rate (R) is set to 0.75 to study the influence of the rate-rate distribution. The steps of Fig. 8 are repeated and compared with the parameter with a code rate of 0.75 as shown in Fig.9.

It can get the same conclusion as the code rate of 0.5 simulation results through the comparison of the BER curves with a code rate of 0.75 under different optimization strategies. The degree distribution obtained by the EFA optimizing only cannot exhibit a reliable performance in the parallel communication of dual media. The bit error floor characteristics of the degree distribution and the waterfall characteristics obtained by joint optimization are better than that obtained by the WFA optimization. The optimization with the lowest BER adjusts the shape of the curve by changing the degree distribution so that the two curves fit more closely. Therefore, the two curves can still be disjointed under the condition of the worst SNR and the correct decoding can be realized. The above conclusion is basically the same as in the case where the code rate is 0.5. The comparison of the degree distributions obtained through algorithm optimization at different code rates shows that the larger the code rate is, the more the waterfall area lags. The maximum impact of the code rate on the performance of the optimization results is the waterfall area. Therefore, the code rate can be adjusted appropriately according to the actual SNR of the power line-wireless parallel channel to utilize the channel resources fully to deliver the corresponding information.

In Fig. 10 the red, blue, and black curves are the BER curves of the joint optimization degree distributions in different channel conditions. With the increasing of probability of noise, the error floor raises and the waterfall area moves to right. When the m of Nakagami-m decreases, the fading of channel becomes stronger. However, the fading of wireless channel do not change the waterfall area. The enhancement in fading of wireless channel raises the error floor only. In summary, the impulse noise has considerable impact on the final decoding result in the power line wireless parallel channel, while the fading has less effect on the decoding than impulse noise. This is because we have used separate transmission and centralized processing to process the information. Diversity technology is an anti-fading technique so

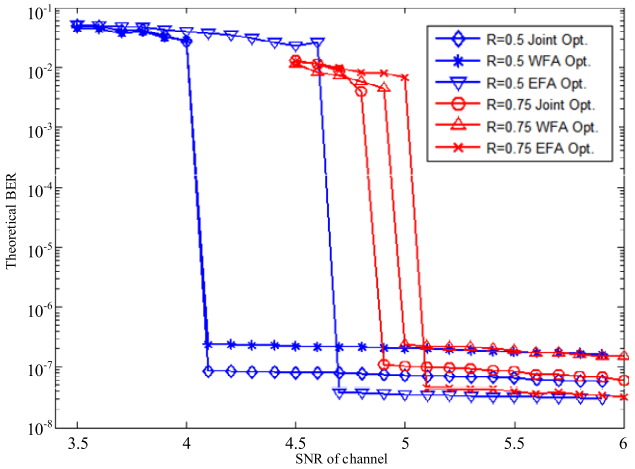

FIGURE 9. BER graph for codes with code rates of 0.5 and 0.75.

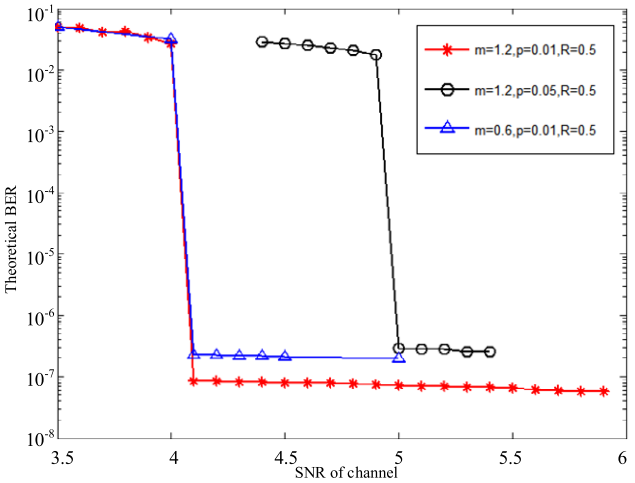

FIGURE 10. Error rates of joint Opt.degree distributions in different channel conditions.

that it is insensitive to the changes in the fading parameters of the wireless channel. The diversity technique can't effectively eliminate the impulse noise, so the impulse noise probability has a great impact on the system.

The iterative progressive performance of the degree distribution can be analyzed through (28). The BER analysis chart under the three-dimensional model clearly shows that the variable node produces mutual information and checks the relationship between the node output mutual information and BER while reflecting the decoding trajectory, as shown in Fig. 11.

The curved surface in Fig. 11 represents the theoretical BER of the joint optimization degree distribution when the impulse noise occurrence probability is 0.05, the SNR is 5 dB. And the orange curve refers to the decoding iteration path of the joint optimization degree distribution. The points on the curve reflect the Iev, Iec and BER information in the iterative process. The red curve represents the decoding iteration path of the optimization degree distribution when the impulse noise occurrence probability is 0.01. The corresponding rounds, Iev, Iec and BER can be found more

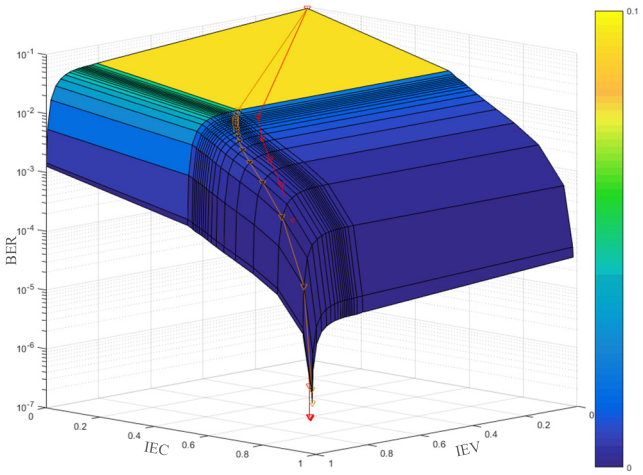

FIGURE 11. Three-dimensional EXIT decoding curves with impulse noise occurrence probabilities of 0.01 and 0.05.

accurately in each iteration through the three-dimensional map.

VI. CONCLUSION

An EXIT algorithm based on Gaussian mixture coding and multi-dimensional node information calculation is proposed in this paper. Gaussian mixture model estimation of the decoding initialization information is performed by the expectation maximized algorithm. Then, the multi-dimensional information processing is performed on the variable node and the check node information in the traditional EXIT algorithm based on the multi-dimensional Gaussian mixture model and system symmetry analysis. Finally, the objective function of LDPC code optimization is constructed. The improved formula, multi-dimensional EXIT chart, optimization algorithm, and three-dimensional error rate map provide necessary solutions for the future analysis of dual media cooperative channels. At present, the key point we studied is the joint optimization in parallel communication system. In future we will study LDPC performance analysis methods and codeword optimization issues in Bi-directional Relays system.

APPENDIXES

APPENDIX A

Mutual information ($I(X|L)$) between the random variable X and the LLR message L is defined as follows:

$$\begin{aligned} I(X|L) &= H(X) - H(H|L) \\ &= 1 - E\left[\log_2\left(\frac{1}{p_{X|L}(x|l)}\right)\right] \\ &= 1 - \sum_{x=\pm 1}\int_{-\infty}^{+\infty} p_{L,X}(l,x)\cdot\log_2\left(1/p_{X|L}(x|l)\right)dl \\ &= 1 - \sum_{x=\pm 1}\int_{-\infty}^{+\infty} p_X(x)\,p_{L|X}(l|x) \\ &\quad \times \log_2\left(\frac{\sum_{x=\pm 1} p_X(x)\cdot p_{L|X}(l|x)}{p_X(x)\cdot p_{L|X}(l|x)}\right)dl \end{aligned}$$

$$= 1 - \sum_{x=\pm 1} \int_{-\infty}^{+\infty} \frac{1}{2} \cdot p_{L|X}(l|x) \times \log_2 \left(\frac{p_{L|X}(l|+1) + p_{L|X}(l|-1)}{p_{L|X}(l|x)} \right) dl$$
$$= 1 - \frac{1}{2} \left\{ \int_{-\infty}^{+\infty} \left[p_{L|X}(l|+1) \cdot \log_2 \left(1 + \frac{p_{L|X}(l|-1)}{p_{L|X}(l|+1)} \right) + p_{L|X}(l|-1) \cdot \log_2 \left(1 + \frac{p_{L|X}(l|+1)}{p_{L|X}(l|-1)} \right) \right] dl \right\}$$

According to the symmetry of message density $p_{L|X}(l|+1) = p_{L|X}(l|-1)$, the above formula can be written as

$$I(X|L) = 1 - \int_{-\infty}^{+\infty} p_L(l|+1) \cdot \log_2 \left(1 + \frac{p_{L|X}(l|-1)}{p_{L|X}(l|+1)} \right) dl$$
$$= 1 - \int_{-\infty}^{+\infty} p_L(l|+1) \times \left[\frac{\exp\left(\frac{-(l-\mu_-)^2}{2\sigma_-^2} \right)}{\exp\left(\frac{-(l-\mu_+)^2}{2\sigma_+^2} \right)} \right] dl.$$
$$= J'(\mu, \sigma)$$

Given that the research object is the component l of the Gaussian-fitted LLR, l satisfies the Gaussian distribution and the variance has a mean. In the above formula, μ_+ represents the mean of l when $X = +1$, μ_- represents the mean of l when $X = -1$, σ_+^2 represents the variance of l when $X = +1$, and σ_-^2 represents the variance of l when $X = -1$. In the simulation, we have verified the symmetry of the system, so $\mu_+ = -\mu_-$, $\sigma_+^2 = \sigma_-^2$. Therefore, it can be simplified as

$$J(\mu, \sigma) = 1 - \int_{-\infty}^{+\infty} p_L(l|+1) \cdot \log_2 \left[\exp\left(-\frac{2\mu l}{\sigma^2} \right) \right] dl.$$

In the above formula, μ is the mean of the LLR message when $X = +1$ is sent and σ^2 is the variance of the LLR message when $X = +1$ is transmitted.

APPENDIX B

$$\exp(-s) = 2 \int_0^{\infty} p_0(x) \exp\left(-\frac{x}{2} \right) dx$$
$$= \sum_{q=1}^{Q} \omega_q \left[\frac{2}{\sigma_q \sqrt{2\pi}} \int_0^{\infty} \exp\left(-\frac{(x-\mu_q)^2}{2\sigma_q^2} \right) \exp\left(-\frac{x}{2} \right) dx \right]$$
$$= \sum_{q=1}^{Q} \omega_q \left[\frac{2}{\sigma_q \sqrt{2\pi}} \int_0^{\infty} \exp\left(-\frac{x^2 - 2\mu_q x + \mu_q^2 + \sigma_q^2 x}{2\sigma_q^2} \right) dx \right]$$
$$= \sum_{q=1}^{Q} \left[\frac{2\omega_q}{\sigma_q \sqrt{2\pi}} \cdot \exp\left(-\frac{\mu_q^2}{2\sigma_q^2} \right) \times \int_0^{\infty} \exp\left(-\frac{1}{2\sigma_q^2} x^2 - \frac{\sigma_q^2 - 2\mu_q}{2\sigma_q^2} x \right) \right] dx$$
$$= \sum_{q=1}^{Q} \left[\frac{2\omega_q}{\sigma_q \sqrt{2\pi}} \cdot \exp\left(-\frac{\mu_q^2}{2\sigma_q^2} \right) \times \int_0^{\infty} \exp\left(-\frac{x^2 + \sigma_q^2 - 2\mu_q}{2\sigma_q^2} x \right) dx \right]$$
$$= \sum_{q=1}^{Q} \omega_q \left[\exp\left(\frac{\left(\sigma_q^2 - 2\mu_q\right)^2 - 4\mu_q^2}{8\sigma_q^2} \right) \times \left[1 - \Phi\left(\frac{\sigma_q^2 - 2\mu_q}{2\sqrt{2}\sigma_q} \right) \right] \right]^{\mathrm{T}}$$
$$= \sum_{q=1}^{Q} \omega_q \left[\exp\left(\frac{\left(\sigma_q^2 - 4\mu_q\right)}{8} \right) \times \left[1 - \Phi\left(\frac{\sigma_q^2 - 2\mu_q}{2\sqrt{2}\sigma_q} \right) \right] \right]$$

The above formula can be calculated according to the following formula:

$$\int_0^{\infty} \exp\left(-\frac{x^2}{4\beta} - \gamma x \right) dx = \sqrt{\pi\beta} \exp\left(\beta\gamma^2 \right) \left[1 - \Phi\left(\gamma\sqrt{\beta} \right) \right], [\mathrm{Re}\beta > 0].$$

APPENDIX C

The Gaussian Hermit formula is

$$\int_{-\infty}^{+\infty} e^{-x^2} f(x)\, dx \approx \sum_{k=0}^{n} A_k f(x_k).$$

For

$$J'(\mu_q, \sigma_q) = \int_{-\infty}^{+\infty} \left(\exp\left(-\frac{(l-\mu_q)^2}{2\sigma_q^2} \right) / \sqrt{2\pi\sigma_q^2} \times \log_2 \left(1 + \exp\left(-\frac{2\mu_q l}{\sigma_q^2} \right) \right) \right) dl$$
$$= \sqrt{2\sigma_q^2} \int_{-\infty}^{+\infty} \left(\exp\left(-(l-\mu_q)^2 / 2\sigma_q^2 \right) / \sqrt{2\pi\sigma_q^2} \times \log_2 \left(1 + \exp\left(-2\mu_q/\sigma_q^2 \times \left[\frac{(l-\mu_q)}{\sqrt{2\sigma_q^2}} \cdot \sqrt{2\sigma_q^2} + \mu_q \right] \right) \right) \right) d\frac{(l-\mu_q)}{\sqrt{2\sigma_q^2}}$$

Let $\frac{l-\mu_q}{\sqrt{2\sigma_q^2}} = z$, then the above formula can be transformed into

$$J'(\mu_q, \sigma_q) = \int_{-\infty}^{+\infty} \left(\frac{1}{\sqrt{\pi}} \exp\left(-z^2 \right) \times \log_2 \left(1 + \exp\left(-2\mu_q/\sigma_q^2 \times \left(z \cdot \sqrt{2\sigma_q^2} + \mu_q \right) \right) \right) \right) dz$$

According to the Gaussian Hermit transformation,

$$J'(\mu_q, \sigma_q) = 1 - \frac{1}{\sqrt{\pi}} \times \sum_{m=1}^{M} (c_m \times \log_2 \left[1 + \exp\left(-2\mu_q/\sigma_q^2 \times \left(\sqrt{2}\, a_m \sigma_q + \mu_q \right) \right) \right]).$$

REFERENCES

[1] V. Fernandes, H. V. Poor, and M. V. Ribeiro, "A hybrid power Line/Wireless dual-hop system with energy harvesting relay," *IEEE Internet Things J.*, vol. 5, no. 5, pp. 4201–4211, Oct. 2018.

[2] M. B. Ghorbel, B. Hamdaoui, M. Guizani, and A. Mohamed, "Long-term power procurement scheduling method for smart-grid powered communication systems," *IEEE Trans. Wireless Commun.*, vol. 17, no. 5, pp. 2882–2892, May 2018.

[3] J. Teh and C.-M. Lai, "Reliability impacts of the dynamic thermal rating system on smart grids considering wireless communications," *IEEE Access*, vol. 7, pp. 41625–41635, 2019.

[4] L. D. M. B. A. Dib, V. Fernandes, M. de L. Filomeno, and M. V. Ribeiro, "Hybrid PLC/Wireless communication for smart grids and Internet of Things applications," *IEEE Internet Things J.*, vol. 5, no. 2, pp. 655–667, Apr. 2018.

[5] F. Salvadori, C. S. Gehrke, A. C. de Oliveira, M. de Campos, and P. S. Sausen, "Smart grid infrastructure using a hybrid network architecture," *IEEE Trans. Smart Grid*, vol. 4, no. 3, pp. 1630–1639, Sep. 2013.

[6] X. Cheng, R. Cao, and L. Yang, "Relay-aided Amplify-and-Forward powerline communications," *IEEE Trans. Smart Grid*, vol. 4, no. 1, pp. 265–272, Mar. 2013.

[7] A. Nosratinia, T. E. Hunter, and A. Hedayat, "Cooperative communication in wireless networks," *IEEE Commun. Mag.*, vol. 42, no. 10, pp. 74–80, Oct. 2004.

[8] Y. Qian, J. Yan, H. Guan, J. Li, X. Zhou, S. Guo, and D. N. K. Jayakody, "Design of hybrid wireless and power line sensor networks with dual-interface relay in IoT," *IEEE Internet Things J.*, vol. 6, no. 1, pp. 239–249, Feb. 2019.

[9] A. Dubey and R. K. Mallik, "PLC system performance with AF relaying," *IEEE Trans. Commun.*, vol. 63, no. 6, pp. 2337–2345, Jun. 2015.

[10] A. Dubey, C. Kundu, T. M. N. Ngatched, O. A. Dobre, and R. K. Mallik, "Incremental selective Decode-and-Forward relaying for power line communication," in *Proc. IEEE 86th Veh. Technol. Conf. (VTC-Fall)*, Toronto, ON, Canada, Sep. 2017, pp. 1–6.

[11] D. Han, S. Li, and Z. Chen, "Hybrid energy ratio allocation algorithm in a Multi-Base-Station collaboration system," *IEEE Access*, vol. 7, pp. 147001–147009, 2019.

[12] K.-H. Kim, H.-B. Lee, Y.-H. Kim, J.-H. Lee, and S.-C. Kim, "Cooperative multihop AF relay protocol for medium-voltage power-line-access network," *IEEE Trans. Power Del.*, vol. 27, no. 1, pp. 195–204, Jan. 2012.

[13] Y.-H. Kim, S. Choi, S.-C. Kim, and J.-H. Lee, "Capacity of OFDM two-hop relaying systems for medium-voltage power-line access networks," *IEEE Trans. Power Del.*, vol. 27, no. 2, pp. 886–894, Apr. 2012.

[14] X. Cheng, R. Cao, and L. Yang, "Relay-aided amplify-and-forward power-line communications," *IEEE Trans. Smart Grid*, vol. 4, no. 1, pp. 265–272, Mar. 2013.

[15] Y. Qian, M. Tian, and X. Jiang, "Performance analysis for a two-way relaying power line networkwith analog network coding," *Frontiers Inf. Technol. Electron. Eng.*, vol. 16, no. 1, pp. 892–898, Apr. 2015.

[16] C. Abou-Rjeily, "Performance analysis of power line communication systems with diversity combining under correlated lognormal fading and Nakagami noise," *IET Commun.*, vol. 11, no. 3, pp. 405–413, Feb. 2017.

[17] A. Dubey, R. Schober, and R. K. Mallik, "Performance analysis of a multi-hop power line communication system over log-normal fading in presence of impulsive noise," *IET Commun.*, vol. 9, no. 1, pp. 1–9, Jan. 2015.

[18] S. W. Lai and G. G. Messier, "The wireless/power-line diversity channel," in *Proc. IEEE Int. Conf. Commun.*, Cape Town, South Africa, May 2010, pp. 1–5.

[19] S. W. Lai and G. G. Messier, "Using the wireless and PLC channels for diversity," *IEEE Trans. Commun.*, vol. 60, no. 12, pp. 3865–3875, Dec. 2012.

[20] J.-H. Lee and Y.-H. Kim, "Diversity relaying for parallel use of power-line and wireless communication networks," *IEEE Trans. Power Del.*, vol. 29, no. 3, pp. 1301–1310, Jun. 2014.

[21] Z. Chen, L. Wang, D. Han, and H. Zeng, "A unified performance analysis of relaying communication system for IoT application with hybrid fading," *IEEE Internet Things J.*, vol. 7, no. 1, pp. 570–583, Jan. 2020, doi: 10.1109/JIOT.2019.2951179.

[22] L. Dai, J. Fu, and J. Wang, "LDPC coded TDS-OFDM for PLC systems," *Tsinghua Sci. Technol.*, vol. 15, no. 3, pp. 312–318, Jun. 2010.

[23] V. Oksman and S. Galli, "G.Hn: The new ITU-T home networking standard," *IEEE Commun. Mag.*, vol. 47, no. 10, pp. 138–145, Oct. 2009.

[24] S. Jayasooriya, M. Shirvanimoghaddam, L. Ong, G. Lechner, and S. J. Johnson, "A new density evolution approximation for LDPC and multi-edge type LDPC codes," *IEEE Trans. Commun.*, vol. 64, no. 10, pp. 4044–4056, Oct. 2016.

[25] B. Dai, R. Liu, Y. Hou, L. Zhao, and Z. Mei, "EXIT chart aided LDPC code design for symmetric alpha-stable impulsive noise," *IEEE Commun. Lett.*, vol. 21, no. 3, pp. 464–467, Mar. 2017.

[26] Z. Mei, M. Johnston, S. Le Goff, and L. Chen, "Performance analysis of LDPC-coded diversity combining on Rayleigh fading channels with impulsive noise," *IEEE Trans. Commun.*, vol. 65, no. 6, pp. 2345–2356, Jun. 2017.

[27] M. N. Khan and M. Jamil, "EXIT chart behaviour for the hybrid FSO/RF communication system," in *Proc. 10th Int. Conf. Inf., Commun. Signal Process. (ICICS)*, Singapore, Dec. 2015, pp. 1–5.

[28] T. Akino and C. Duan, "Optical communications network and method for adaptively coding signals in optical network," WO Patent 201 4077 139 A1, May 22, 2014. [Online]. Available: https://patents.google.com/patent/WO2014077139A1/en

[29] A. Roumy and D. Declercq, "Characterization and optimization of LDPC codes for the 2-user Gaussian multiple access channel," *EURASIP J. Wireless Commun. Netw.*, vol. 2007, no. 1, pp. 9–10, Dec. 2007.

[30] S. Sharifi, A. K. Tanc, and T. M. Duman, "LDPC code design for the two-user Gaussian multiple access channel," *IEEE Trans. Wireless Commun.*, vol. 15, no. 4, pp. 2833–2844, Apr. 2016.

[31] N. Zheng, Y. He, B. Bai, A. M.-C. So, and K. Yang, "LDPC code design for Gaussian multiple-access channels using dynamic EXIT chart analysis," in *Proc. IEEE Int. Conf. Acoust., Speech Signal Process. (ICASSP)*, New Orleans, LA, USA, Mar. 2017, pp. 3679–3683.

[32] G. J. Byers and F. Takawira, "EXIT charts for non-binary LDPC codes," in *Proc. IEEE Int. Conf. Commun. (ICC)*, Seoul, South Korea, vol. 1, May 2005, pp. 652–657.

[33] M. Stinner and P. M. Olmos, "On the waterfall performance of finite-length SC-LDPC codes constructed from protographs," *IEEE J. Sel. Areas Commun.*, vol. 34, no. 2, pp. 345–361, Feb. 2016.

[34] S. Wahane, S. Kakde, A. Khobragade, and W. Elmedany, "A systematic approach for achieving low bit error rate of LDPC decoder using MWD algorithm," in *Proc. Int. Conf. Wireless Commun., Signal Process. Netw. (WiSPNET)*, Chennai, India, Mar. 2017, pp. 29–33.

[35] J. Bao, B. Jiang, and C. Liu, "Optimized construction of protograph G-LDPC codes by modified EXIT chart and MACE for new-generation wireless communications," *IEEE Access*, vol. 6, pp. 58139–58153, 2018.

[36] Z. Chen, D. Han, and L. Qiu, "Research on the performance of indoor wireless and power line dual media cooperative communication system," *Proc. CSEE*, vol. 37, no. 9, pp. 2589–2598, May 2017.

[37] S. Zhang, C. Tsimenidis, H. Cao, and S. Boussakta, "Coded OFDM in PLC channels with SaS distribution impulsive noise using MRC detector," in *Proc. U.K./ China Emerg. Technol. (UCET)*, Glasgow, U.K., Aug. 2019, pp. 1–4.

[38] Y. Jung, Y. Jung, S. Lee, and J. Kim, "Low-complexity multi-way and reconfigurable cyclic shift network of QC-LDPC decoder for Wi-Fi/WIMAX applications," *IEEE Trans. Consum. Electron.*, vol. 59, no. 3, pp. 467–475, Aug. 2013.

ZHIXIONG CHEN was born in Fujian, China, in 1983. He received the master's degree from the Harbin Institute of Technology of China, in 2007, and the Ph.D. degree in electrical engineering and its automation from the North China Electric Power University, China, in 2010. He is currently an Associate Professor with the North China Electric Power University. His main research interest includes power system communication.

YU GU was born in Henan, China, in 1994. He received the B.S. degree in communication engineering from North China Electric Power University, in 2017, where he is currently pursuing the M.S. degree in electrical and electronic engineering. His main research interests include wireless cooperative communication and channel coding.

PEIRU CHEN was born in Urumqi, China, in 1996. She received the B.S. degree in communication engineering from North China Electric Power University, in 2019, where she is currently pursuing the M.S. degree in electrical and electronic engineering. Her main research interest includes wireless cooperative communication.

JINGXI ZHANG was born in Luoning, Henan, China, in 1973. He received the B.S. degree in information engineering from the Chengdu Institute of Technology, in 1997, and the M.S. and Ph.D. degrees in communication engineering from the Beijing University of Postal and Telecommunications, in 2005 and 2011, respectively. He is currently a Lecturer with the School of Electrical and Electronic Engineering, North China Electric Power University. His research interests include wireless communication, coding theory and its applications, and broadband wireless communication.

DONGSHENG HAN was born in Qiqihar, China, in 1980. He received the Ph.D. degree in communication and information system from Beijing Jiaotong University, China, in 2012. He is currently an Associate Professor with North China Electric Power University. His main research interests include digital communication systems and wireless communication.